International Journal of Engineering Technology Science and Research
IJETSR
www.ijetsr.com
ISSN 2394 – 3386
Volume 4, Issue 4
April 2017

Brain Tumor Segmentation Using MS Algorithm

Mr. Vilas P. Salve
Dept. of Computer
SRTM University,
Nanded.

Ms. Amrapali K. Salve
Dept. of ECT
MGM's College of Engg.,
Nanded.

Dr. Ms. K. C. Jondhale
Dept. of ECT
MGM's College of Engg.,
Nanded.

ABSTRACT

In this paper we developed Brain tumor techniques using tomography, such as MRI (Magnetic Resonance images) provide a plethora of pathophysiological tissue information that assists the clinician in diagnosis, therapy design/monitoring and surgery. Robust segmentation of brain tissues is a very important task in order to perform a number of computational tasks including morphological measurements of brain structures, automatic detection of asymmetries and pathologies, and simulation of brain tissue growth. In this paper we present brain structure segmentation results based on our implementation of the mean-shift algorithm and compare them with a number of well-known brain-segmentation algorithms using an atlas dataset as ground truth. The results indicate that the mean-shift algorithm outperforms the other methods. Last, the value of this algorithm in automatic detection of abnormalities in brain images is also investigated.

Index Terms— Mean Shift Algorithm (MSA), K-Mean Clustering (KMC), Markov Random Fields (MRF), Image Segmentation.

I. INTRODUCTION

Magnetic resonance imaging (MRI) is a widely used imaging technique to assess tumors, but the large amount of data produced by MRI prevents manual segmentation in a reasonable time, limiting the use of precise quantitative measurements in the clinical practice Magnetic resonance images (MR images) of the brain are acquired using different protocols, e.g. T 1 weighted images with contrast enhancement of the active tumor region and T2 weighted images. In order to be able to make use of the acquired images, different regions in the images have to be delineated. The regions of interest usually correspond to the different tissue types, which are present in the brain. Clustering brain pixels into one of three main brain tissue types (Cerebrospinal fluid, Gray Matter, White Matter) proves to be of paramount importance in anticipation and treatment of various diseases, such as multiple sclerosis, Alzheimer's disease or epilepsy. Numerous segmentation methods have been proposed for this task, following either supervised or unsupervised approaches [1].

Supervised classification requires input from the user, typically a set of pixel class samples. The authors in [2], in order to classify CSF, GM, WM and brain lesions use a k-NN classifier, followed by a connected components filtering algorithm for result refinement. Other classifiers that have been used for brain tissue classification include discriminative Random Decision Forest classification [3] .

On the other hand, unsupervised approaches often rely on a Gaussian approximation of the pixel intensity distribution for each tissue type. An example of the use of Gaussian mixture models is introduced in [5], where the authors also employ a probabilistic brain atlas as a prior. An additional unsupervised method has been created, which models neighboring pixels interactions using a Markov-Random field (MRF) statistical model [6].

An alternative to statistical parametric approaches is the use of unsupervised, nonparametric schemes. One such approach is the Mean-shift algorithm [7], which uses adaptive gradient ascent in order to detect local maxima of data density in feature space. This approach is followed in [8], producing promising results, without the use of a statistical brain atlas.

The brain tissue segmentation could also be a first step for the detection of tumor cells or other tissue abnormalities. Interpretation of the radiological evolution of the tumor appears of utmost importance for therapeutic management, e.g. in the case of low-grade glioma. Many automated or semi-automated approaches were developed over the past ten years showing great variability in results and performance in terms of reproducibility. Challenges in the segmentation of gliomas from MRI data are related to i) the infiltration of cells into the tissue, inducing unsharp borders with irregularities and discontinuities (a tumor is not necessary a single connected object), ii) the great variability in their contrast uptake (depending on their vascularisation) and iii) their appearance on standard MRI protocols,

International Journal of Engineering Technology Science and Research
IJETSR
www.ijetsr.com
ISSN 2394 – 3386
Volume 4, Issue 4
April 2017

especially Tl-weighted enhanced (Tl E) with contrast agent (usually Gadolinium), and T2-weighted (e.g. FLAIR) data. The majority of the MRI-based glioma segmentation methods that have been proposed in the literature are regionbased. More recent methods, based on deformable models, also included edge-based information.

In this paper we compare brain tissue clustering with KMeans, Markov Random Fields (MRFs) and Gaussian Mixture Model (GMM) and our own implementation of the mean-shift algorithm, which follows the main lines of [8]. We also investigate the use of mean-shift algorithm in automatic detection of tumor in brain images.

II. METHODS

In this section we describe the four well-known methods for brain tissue classification that we apply in our Comparative study:

A. *Clustering using the Classical K-Means*

The k-means algorithm [9], [10] is a fast and easy iterative clustering technique, used to cluster a given dataset into a specific number of K clusters, so as to minimize the sum-of squares objective function :

$$J = \sum_{j=1}^{m}\sum_{i=1}^{n}\left\| x_i^{(j)} - c_j \right\|^2 \qquad (1)$$

Where, $\left\| x_i^{(j)} - c_j \right\|^2$ is the squared Euclidian distance between the data point $x_i^{(j)}$ and the cluster center c_j, k is the number of clusters and n is the number of data points. The k-means algorithm updates the clusters of the input data iteratively, while the elements of the data are exchanged between the clusters, based on the minimization of the aforementioned predefined function.

The classical K-Means clustering algorithm consists of the following four steps:

1. Initialization - Define the number of clusters, as well as the initial cluster centers
2. Assign each data point to the nearest cluster center
3. Recalculate the centers of the new clusters
4. Repeat steps 2 and 3 until a distance convergence
5. criterion is met

B. *MSA(Mean- Shift Algorithm)*

Let $x_i, i = 1,2,3,.....,n,$ where n is the total amount of brain pixels of the MRI photo, in the $d = 3$ dimensional space R^3 ($x - y$ spatial information and I intensity information). The density at point x can be estimated by the Parzen window Kernel density estimator:

$$f_k(x) = \frac{1}{n}\sum_{i=1}^{n}\frac{1}{h_i^{\,d}}k\left(\left\|\frac{x - x_i}{h_i}\right\|^2\right) \qquad (2)$$

Where, k is he profile of the spherically symmetric kernel K, with bounded support that satisfies $K(x) = c_{k,d}k(\|x\|^2) > 0, \|X\| <= 1, c_{k,d}$ is a normalization constant that makes K (x) integrate to one, and h_i is the kernel bandwidth and determines the range of influence of the kernel located in x_i. In this work, h_i is chosen to be the distance between x_i and its k-nearest neighbor, $x_{i,k}$ and the normal kernel $K(x) = \exp(-\|x\|^2)$ is used.

Provided that the $k'(x)$ exists, then $g(x) = -k'(x)$ can be defined with the associated kernel $G(x) = c_{g,d}\,g(\|x\|^2)$, which here has the same expression as K (x) , since we use the normal kernel. The gradient of (2) leads to:

$$C\frac{\Delta f_k(x)}{f_G(x)} = \frac{\sum_{i=1}^{n}\frac{1}{h_i^{\,d+2}}x_i \exp\left(-\left\|\frac{x - x_i}{h_i}\right\|^2\right)}{\sum_{i=1}^{n}\frac{1}{h_i^{\,d+2}}\exp\left(-\left\|\frac{x - x_i}{h_i}\right\|^2\right)} - x \qquad (3)$$

Where C is a positive constant and the right-hand side is the mean-shift vector. Since the mean-shift vector is proportional to the normalized gradient of the density estimate computed for kernel, the mean-shift vector points towards the direction of the maximum density increase [11]. Starting from point y_j in feature space, we move with the mean-shift vector to a point y_{j+1} that lies in a higher density region than y_j , computed as follows:

$$m_{h,N} = y_{j+1} - y_j$$

International Journal of Engineering Technology Science and Research
IJETSR
www.ijetsr.com
ISSN 2394 – 3386
Volume 4, Issue 4
April 2017

$$m_{h,N}(y_{j+1}) = \frac{\sum_{i=1}^{n} \frac{1}{h_i^{d+2}} x_i \exp\left(\left\| \frac{y_j - x_i}{h_i} \right\|^2\right)}{\sum_{i=1}^{n} \frac{1}{h_i^{d+2}} \exp\left(\left\| \frac{y_j - x_i}{h_i} \right\|^2\right)} - y_j \quad (4)$$

We can also deduce from (3) that the mean-shift vector length is modulated by the inverse of the kernel density estimation with kernel G. Therefore, as we move towards higher density regions along the mean-shift vector, its length gradually decreases. By repeating iteratively, we progressively climb to the nearest stationary point of the probability density function which is usually also one of its local maxima. The decrease in norm of the mean-shift vector between successive iterations can be used as a convergence criterion to stop the iterations. The above procedure is executed for every brain pixel of the MR image. Then, we search in small neighbors for the local maxima of the stationary points that we calculated with (4) for every pixel, thus defining the modes. The classification of every pixel follows, using Euclidean distance, according to the nearest mode [7], [8]. If the number of the remaining modes is large (>400) we prune the modes with a Mahalanobis classifier, using only intensity information, until the remaining modes are only a few hundreds. In our implementation, when the pruned remaining modes reach the limit of 400 the algorithm proceeds to the next phase, while in [8] merging continues until the largest variance among all pruned modes exceeds a preset threshold and also the minimum allowed number of the remaining modes is 100. In the final phase, the remaining modes are classified to the three brain tissues, according to the fuzzy k-means algorithm, instead of the classical Kmeans, used in [8]. Other differences between our implementation and the original mean-shift algorithm include the use of the Gaussian kernel instead of the Epanechnikov, for the calculation of the mean-shift vector, as well as the output of the algorithm as both a segmentation map for all pixels and a membership matrix which contains the probability for every pixel to belong to each one of the three main brain tissues, instead of only a segmentation map.

C. Clustering with Markov Random Fields (MRF)

The MRF [12], [13] is a stochastic process, used as a priori model to incorporate spatial correlations into a segmentation Ilabeling process. It is used to label pixels of a two-dimensional image lattice $S = \{1,....,n\}$. In that lattice, the pixel values $y = \{y_1,....,y_n\}$ are assumed to be a realization of the random variables $x = \{x_1,....,x_n\}$

An optimal labeling of the MRF satisfies the maximum a posteriori probability criterion (MAP-MRF), which requires the maximization of the posterior probability P(x | y) of the labeling. Assuming that P(x | y) follows the Gibbs distribution [13], and utilizing the simplified Bayes rule P(x|y)α P(x)p(y|x) , the posterior probability can be expressed in terms of the posterior energy, as the sum of the prior and the likelihood energy term:

$$U(x|y) = U(x) + U(y|x) \quad (5)$$

The Gibbs distribution model defines the labeling of a pixel in dependence to the labeling of all the other pixels of the lattice S. However, the MRF model is a conditional probability model, where the probability of a pixel label depends on the pixel labels within its neighborhood.

The equivalence of the Gibbs and the MRF models is stated in the Hammersley-Clifford theorem. The prior and likelihood energies can be expressed in terms of potentials of cliques, which are groups of neighboring pixels, whose order (that indicates the number of included pixels) is variable, according to the desired complexity .

The MAP-MRF solution is equivalent to the minimization

of the energy, as defined in (5):

$$x = \arg\min U(x|y) \quad (6)$$

In order to find the global minimum of that energy, in this work, the deterministic iterated-conditional mode algorithm

(lCM) [12] was used.

Table No.1 Comparison of Classification algorithm

Sr. No.	Clustering Algo.	Tissue Type	Sensitivity	DSC	Tanimoto Coefficient
1	K-Mean	CSF	0, 85	0, 77	0, 94
		GM	0, 75	0, 81	0, 92
		WM	0, 90	0, 84	0, 95
2	Mean-Shift	CSF	0, 89	0, 83	0, 96

International Journal of Engineering Technology Science and Research
IJETSR
www.ijetsr.com
ISSN 2394 – 3386
Volume 4, Issue 4
April 2017

		GM	0, 82	0, 86	0, 94
		WM	0, 91	0, 87	0, 96
3	MRF	CSF	0, 45	0, 59	0, 93
		GM	0, 49	0, 55	0, 85
		WM	0, 93	0, 69	0, 89

*MRF=Markov Random Fields, DSC=Dice Similarity Coefficient, CSF= Cerebrospinal Fluid, GM=Grey Matter, WM= White Matter.

III. RESULT S

A. Evaluation based on pre-Segmented MR Brain Atlas

In order to evaluate the efficiency of the four algorithms previously described, in respect to brain tissue classification

in MR we used the SRl24 atlas [16], which is an

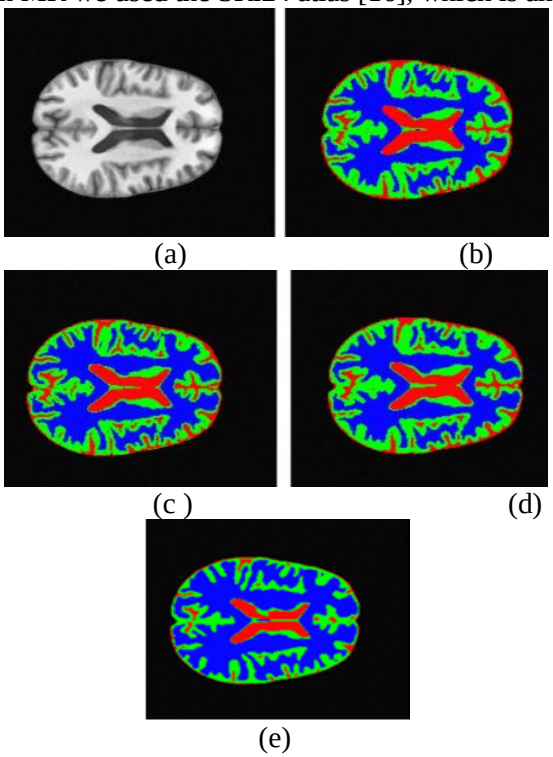

(a) (b) (c) (d) (e)

Fig. 1 (a) Tl slice form SRl24 atlas, (b) Labeled atlas image, (c) Clustering result with K-Means, (d) Clustering result with Mean-Shift, (e) Clustering result with Markov Random Field,

MRI-based atlas of normal adult brain anatomy, generated by template-free non rigid registration from images of 24 normal control subjects. The atlas includes Tl, T2 and PO weighted MR images, as well as pre-labeled maps of the tissues of interest (WM, GM, CSF).

Each of the four algorithms was applied on a set of 120 anatomical images of the Tl atlas series. The K-Means and MRF algorithms were implemented using the corresponding functions of the open-source segmentation and registration toolkit ITK 3. 16, while Mean-Shift and GMM were implemented using Matlab. The results of K-Means were

used as an initialization of the cluster centers of the MRF, as well as an initialization of the means and covariances of each component of the GMM. In every case, the number of clusters was pre-set to three.each algorithm. Table I shows the calculated sensitivities, Dice Similarity Coefficient (DSC) [17], and Tanimoto Coefficient [1 8], for each one of the four algorithms and for each one of the brain tissues., while Fig.l illustrates a slice of the Tl atlas series, as well as the corresponding prelabeled atlas image, along with the results of the application of the four algorithms on that image.

B. Application in Real case: MR Images of Brain Tumor

The Mean-Shift clustering algorithm, in combination with prior knowledge about the nature of the Tl and T2 MR Images can be used, not only to classify the various brain tissues, but also to detect possible cancer cells. Because of the nature of the enhanced Tl-weighted modality, the tumor necrotic area appears hypointense, while the solid area of the tumor around the necrotic area appears hyperintense and the edema cannot be distinguished from the GM and the WM, which both share medium intensities. Similarly, in T2-flair images, the edema and the solid tumor area appear hyperintense, while the necrotic area appears hypointense. An example of these two modalities is shown in Fig. 2 (a) and (b), where the skull has been removed manually from the two registered images.

Using that information, we can perform clustering on two corresponding registered Tl-enhanced and T2-flair images, using 4 clusters. After identifying the cluster with the higher mean value, since it is the most probable to include the tumor region, we remove the connected components having area below a certain threshold. The largest connected component will be most likely the tumor area, in both MR modalities. If we subtract the tumor area of

International Journal of Engineering Technology Science and Research
IJETSR
www.ijetsr.com
ISSN 2394 – 3386
Volume 4, Issue 4
April 2017

Tl from the tumor area of T2-flair, then we obtain the edema region.

An example of this is shown in Fig. 2 (c), where the tumor area obtained from Tl (after morphological closing, in order to include the necrotic area, as well) is highlighted with green, superimposed on the original image, while in (d) the edema is also shown with blue, superimposed on the T2-flair image.

IV. DISCUSSION

The results in Table 1 clearly demonstrate that the meanshift algorithm yields the most accurate segmentation results for brain tissue segmentation based on the SRI24 Atlas validation performed in all tissue types based on the DSC and Tanimoto Coefficient measures. The MRF method didn't perform as expected mainly exhibiting a very low sensitivity in segmenting correctly the different brain tissue types with the exception of WM where it outperformed the other methods. It should be noted that only the Tl images were taken into consideration in these experiment and future work should expend this comparison to all modalities that are available for each patient. The same method was used for

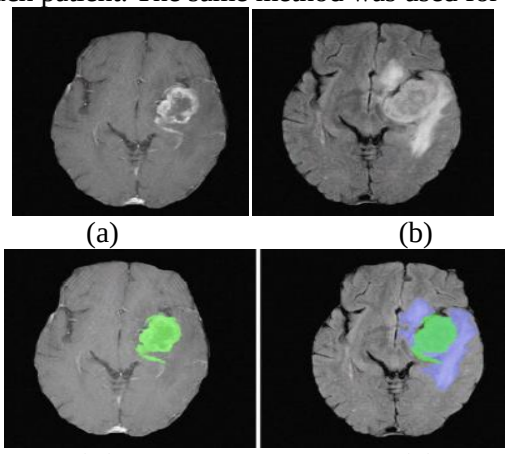

Fig. 2 (a) Enhanced Tl-weighted image after the skull has removed, (b) Corresponding registered T2-flair image, (c) Solid tumor area obtained from enhanced Tl, (d) Solid tumor area and edema obtained from T2-flair.

preliminary results in tumor/edemal tissue identification, a very crucial task for the on cologist. The initial results are very promising but a detailed validation work on this should be carried out in the future. Additionally, since the brain structures usually appear very symmetric, a high level of asymmetry, around an axis of symmetry would strongly indicate some kind of abnormality (tumor, edema, cysts, etc.). Such information can be incorporated in order to refine the tumor detection and segmentation result.

V. CONCLUSION

This paper presented a comparison of four well-known brain tissue segmentation techniques including our implementation of the mean-shift algorithm based on an atlas dataset as ground truth. The results indicate that the mean-shift algorithm outperforms the other methods and can be potentially used for identifying abnormalities in brain images (e.g. in the case of glioma). Future work including more experiments is needed to establish these results.

ACKNOWLEDGMENT

The authors would like to thank Dr. A. Tapdiya and pathologist Dr. Rashmi Parsewar at sanjeevani Hospital Nanded MH, India for her valuable clinical guidance in this work.

REFERENCES

[1] D. L. Pham, C. Y. Xu, and J. L. Prince, "A survey of current methods in medical image segmentation," *Annu. Rev. Biomed. Eng.*, vol. 2, pp. 315-337,2000

[2] R. Cardenes, S. K. Warfield, E. M. Macias, J. A. Santana, and 1. RuizAlzola, "An efficient algorithm for mUltiple sclerosis segmentation from brain MRI," *in Int. Workshop Comput. Aided Syst. Theory (EUROCAST),* pp. 542-551, 2003

[3] Yi, A. Crimi nisi, 1. Shotton, and A. Blake, "Discriminative, semantic segmentation of brain tissue in MR images," *in Int. Conf. Med. Image Compo Assist. Int. (MICCAI),* pp. 558-565,2009.

[4] R. P. Agiula, "Automatic segmentation and classification of computed tomography brain images: An approach using one-dimensional Kohonen networks," *Int. J. Compo Science*, vol. 37,2010.

[5] G. Dugas-Phocion, M. A. Gonzalez Ballester, G. Malandain, C.Lebrun, and N. Ayache, "Improved EM-based tissue segmentation and partial volume effect quantification in multi-sequence brain MRI," *in Int. Conf. Med. Image Compo Assist. Int. (MICCAI),* pp. 26-33, 2004.

[6] K. Van Leemput, F. Maes, D. Vandeurmeulen, and P. Suetens, "Automated model-based tissue classification of MR images of the brain," *IEEE Trans. Med. Imag.*, vol. 18, pp. 897-908,1999.

[7] D. Comaniciu and P. Meer, "Mean-shift: A robust approach toward feature space analysis," IEEE Trans. Pattern Anal. Mach. Intell., vol. 24,pp.603-619,2002.

[8] Arnaldo Mayer and Hayit Greenspan, "An adaptive Mean-shift Framework for MRI Brain Segmentation ", *IEEE Trans. Med. Imag.*, vol. 28, pp 1238-1250,2009.

[9] J. MacQueen, "Some methods for classification and analysis of multivariate observations," *Proc. 5th Berkeley Symp. Math. Statist. Prob*. vol. I, pp. 281-297,1967.

[10] M. M. Ahmed, and D. Mohammad, "Segmentation of brain MR images for tumor extraction by combining kmeans clustering and Perona-Malik anistropic diffusion model," *Int. J. Image Proc.*, vol. 2, pp. 27-34,2008.

[11] K. Fukunaga and L. D. Hostetler, "The estimation of the gradient of a density function, with applications in pattern recognition," *lEEE Trans. Inf. Theory*, vol. 21, no. I, pp. 32-40, Jan. 1975.

[12] 1. E. Besag, "Spatial interaction and the statistical analysis of lattice systems," *J. R. Stat. Soc.* vol. B-36, pp. 192-236, 1974.

[13] S. l. Li, "Markov Random Field modeling in Computer Vision," *Springer, New York*, 2001.

[15] A. D. Dempster, N. M. Laird, and D. B. Rubin, "Maximum likelihood from incomplete data via the EM algorithm," *J. R. Stat. Soc.*, vol. 39, pp. 1-38, 1977.